Res Chem Intermed (2016) 42:7991–8004
DOI 10.1007/s11164-016-2574-z

# Synthesis of silver nanoparticles via green method using ultrasound irradiation in seaweed *Kappaphycus alvarezii* media

**Miftah Faried[1] · Kamyar Shameli[1,2] · Mikio Miyake[1] · Ablollah Hajalilou[1] · Katayoon Kalantari[1] · Zuriati Zakaria[1] · Hirofumi Hara[1] · Nurul Bahiyah Ahmad Khairudin[1]**

Received: 21 February 2016 / Accepted: 4 May 2016 / Published online: 10 May 2016


**Abstract** Green methods are a safer alternative to natural chemical and physical methods for the synthesis of silver nanoparticles (Ag-NPs), due to their being environmentally friendly and cost effective. This study offers a new green approach using ultrasound irradiation as the reducing agent and seaweed *Kappaphycus alvarezii* (*K. alvarezii*) as the natural bio-media. The seaweed *K. alvarezii*/Ag-NPs was characterised by ultraviolet–visible (UV–vis), X-ray diffraction (XRD), transmission electron microscopy (TEM), scanning electron microscope with energy dispersive X-ray (FESEM-EDX), zeta potential, and Fourier transform infrared (FTIR) studies. UV–vis shows that surface plasmon resonance (SPR) arises from this solution due to the combined oscillations from the nanoparticles. The XRD study indicates the crystalline nature of the Ag-NPs. From the TEM images, the Ag-NPs are almost spherical with an average diameter of 11.78 nm. The FTIR spectrum provides adequate evidence of phytochemicals stabilising the nanoparticles. Synthesised Ag-NPs were successfully obtained using this green method.

**Keywords** Silver nanoparticles · Green method · Seaweed *Kappaphycus alvarezii* · Ultrasound irradiation

✉ Kamyar Shameli
kamyarshameli@gmail.com

[1] Department of Environment and Green Technology, Malaysia-Japan International Institute of Technology, Universiti Teknologi Malaysia, Jalan Sultan Yahya Petra, 54100 Kuala Lumpur, Malaysia

[2] Department of Nanotechnology and Advance Materials, Materials and Energy Research Center, P.O. Box: 31787-316, Karaj, Alborz, Iran

## Introduction

Nanotechnology is a relatively new technology dealing with tolerances ranging from 1 to 100 nm, and can be used in a broad range of fields including chemistry, physics, and biology [1, 2]. Because of their unique material properties, nanotechnology is one of the most active research areas in modern science and engineering. It has technological applications, such as for catalysis [3], sensors [4], and antimicrobials [5].

Today, the synthesis of nanoparticles and their self-assembly is a fundamental concept in nanotechnology. Much of this synthesis contains environmental risks due to chemical reagents. Hence, new eco-friendly methods in the synthesis of nanoparticles are being developed. One famous type of metal nanoparticle is the silver nanoparticle (Ag-NP), due to its physicochemical properties [6]. Ag-NPs have been widely studied and have many applications, such as in anti-microbial agents [7], electromagnetic fields [8], and optical sensors [9].

The synthesis of Ag-NPs is an important aspect of nanotechnology, because of their many applications. However, the synthesis of Ag-NPs usually uses chemical methods such as sodium borohydride, polyvinyl alcohol, and ethylene glycol, which have environmental effects [10]. This paper argues that a green synthesis method of Ag-NPs can be a good alternative to producing Ag-NPs. Ag-NPs can be prepared by green synthesis using irradiation as a reducing agent, such as gamma irradiation [11], ultraviolet (UV) irradiation [12], microwave irradiation [13], and ultrasound irradiation [14].

Ultrasound irradiation is an alternative method for decreasing chemical reagents, with simple, clean, and efficient procedures [15]. in 1992, Nagata et al. [16] were the first to produce stable colloidal silver in aqueous $AgNO_3$ under ultrasound irradiation treatment (20 kHz). Sonication mechanism is known as cavitation, and can produce a radical species by generating bubbles in solution. The bubbles grow in the solution and collapse at high temperature and pressure. This extreme condition can break chemical bonds and allow formation of free radicals [17].

Another part in the green synthesis of Ag-NPs is the use of plant extracts. Several plants have been used to successfully produce Ag-NPs. However, the outcome has been somewhat unstable [18, 19]. Seaweed can be used to solve this problem in the synthesis of Ag-NPs because it has biopolymers from natural resources, such as polysaccharides [20].

The seaweed *Kappaphycus alvarezii* (*K. alvarezii*) is a red tropical seaweed that is economical and in high demand due to it cell wall polysaccharides. It is an most important source of kappa-carrageenan; it is readily available in large quantities and used both for food and pharmaceutical applications [21]. Seaweed *K. alvarezii* has a linear water-soluble sulphated polysaccharides carrageenan widely used as a gelling agent in food and pharmaceutical industries [22]. This seaweed has never before been reported as media for the green synthesis of Ag-NPs under ultrasound irradiation.

In our previous research on synthesising Ag-NPs [23], data have been inconclusive. Ganesan et al. [24] studied producing Ag-NPs using seaweed *K.*

*alvarezii* under incubated shaking for 96 h. Their research is on a novel green synthesis of Ag-NPs using seaweed *K. alvarezii*, by ultrasound method under varying time irradiations. This synthesis is a simple method for quick and facile synthesis of Ag-NPs. The obtained of seaweed *K. alvarezii*/Ag-NPs were characterised by ultraviolet–visible (UV–vis) spectrophotometry, X-ray diffraction (XRD), transmission electron microscopy (TEM), scanning electron microscope with energy dispersive X-ray (FESEM-EDX) spectroscopy, zeta potential analyser, and Fourier transform infrared (FTIR) spectroscopy.

## Materials and methods

All reagents for this research were used as received, without any purification. The seaweed *K. alvarezii*, a kind of red algae, was obtained from Sabah, Malaysia. Silver nitrate ($AgNO_3$) was obtained from Bendosen 99.89 % (C0721-2284551). The purified water was prepared as the solvent from ELGA Lab-Water/VWS (UK) purification system.

### Synthesis of silver nanoparticles

A total of 100 ml $AgNO_3$ 10 mM solution was added to 400 ml of *K. alvarezii* (0.3 wt%). *K. alvarezii* was crushed by a grinder until a uniform suspension was obtained. The solutions were exposed to high-intensity ultrasound irradiation at an amplitude of 70 Hz and 0.5 of a cycle. Fifteen milliliters of the $AgNO_3$/*K. alvarezii* solutions were taken each around after irradiation for 10, 30, 60, 120, 240, 360, 480, 600, and 720 min to study the effect of irradiation times. As the control for this synthesis is *K. alvarezii* media without any treatment radiation, treatment of all samples continued without washing to preserve the wetness of the solution. Ultrasound irradiation was carried out with an ultrasonic liquid processor (Hielscer Ultrasound Technology UP-200S-RN, Germany, 50/60 Hz) with a probe directly immersed into the reaction solution.

### Characterisation methods and instruments

The *K. alvarezii*/Ag-NPs were characterised using ultraviolet–visible (UV–vis) spectroscopy over the range of 300–800 nm with a UV–vis spectrophotometer (UV-1800, SHIMADZU). A powder X-ray diffraction (PXRD) with Cu Kα radiation was used to study the crystallinity of the nanoparticles. The XRD patterns were carried out on a Philips (X'pert, Cu Kα) and were recorded at a scan speed of 2°/min. Transmission electron microscopy (TEM) was recorded using a Tecnai$^{TM}$ G2 F20 Series to study the size of Ag-NPs. Field Emission Scanning electron microscope (FESEM) was carried out on a JEOL-JSM-7600F and energy dispersive X-ray (EDX) was performed with the Philips XL 30 to study the elements of the nanoparticles. Zeta potential using the Particulate Systems Nano-Plus Zeta/Nano Particle Analyser, Japan, was used to record the stability of Ag-NPs. Fourier transform infrared spectroscopy (FTIR) spectra were recorded over the range of 200

to 4000 $cm^{-1}$ with a series Aligent Technologies Cary 660 Series FTIR Spectrometer.

## Results and discussion

The reduction of $AgNO_3$ was visually evident from the changing colour of the solution of the reaction mixture after 720 min of ultrasound irradiation at room temperature. The intensity of colour increased from being colourless to a dark brown with increasing radiation time, as shown in Fig. 1.

The colour changes of these solutions related to the formation of Ag-NPs in the seaweed *K. alvarezii*, and this phenomenon will be clarified with surface plasmon resonance (SPR) in UV–vis spectra.

When the suspension is exposed to ultrasonic irradiation, bubbles grow. After the bubble size reaches the maximum value, the bubbles collapse. This great collapse raises the temperature and causes the rupture of chemical bonds and the formation of free radicals [16, 25, 26]. The mechanism of the colloidal silver formation can be suggested as shown in Eqs. (1–7). After exposing $AgNO_3$/*K. alvarezii* aqueous suspensions to ultrasonic waves, there were primary radicals $H^{\cdot}$ and $OH^{\cdot}$, as described in Eq. (1).

$$nH_2O \xrightarrow{\text{Sonicate}} n(H^{\cdot} + {}^{\cdot}OH) \tag{1}$$

$AgNO_3$ separated to $Ag^+$ and $NO_3^-$ ions in the aqueous solution as shown in Eq. (2).

$$AgNO_3 \xrightarrow{\text{Hydrolesis}} Ag^+ + NO_3^- \tag{2}$$

The indirect effect of OH radicals yielded free radicals inside the polymer groups in Eq. (3), and this free radical was reduced by $Ag^+$ to form Ag° and the new group (R′), as in Eq. (4).

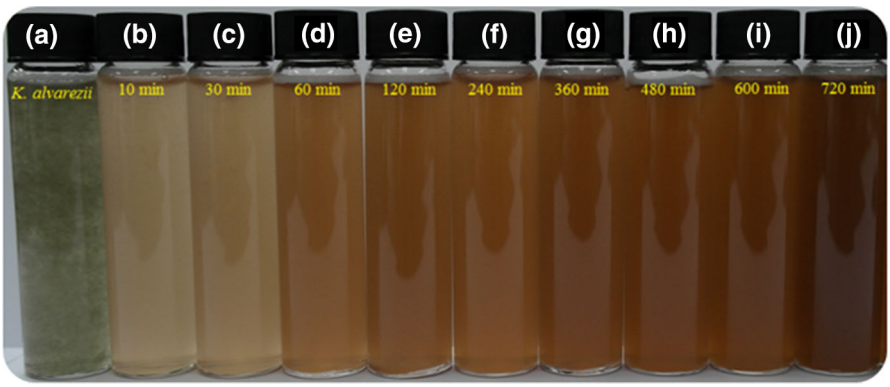


**Fig. 1** Photograph of *K. alvarezii* (**a**) and *K. alvarezii*/Ag-NPs suspension at different ultrasound irradiation times [10, 30, 60, 120, 240, 360, 480, 600, and 720 min (**b–j**)]

$$^{\cdot}OH + RH \rightarrow R^{\cdot} + H_2O \tag{3}$$

$$R^{\cdot} + Ag^{+} \rightarrow Ag^{\circ} + R' + H^{+} \tag{4}$$

Also, $H^{\cdot}$ radicals are a strong reducing agent. They can reduce silver ions to the zero-valent state, as in Eq. (5).

$$H^{\circ} + Ag^{+} \xrightarrow{\text{Reduction}} Ag^{\circ} + H^{+} \tag{5}$$

Equation (6) refers to the direct reaction of $Ag^{+}$ with water in the interfacial region between the cavitation bubbles and the liquid.

$$Ag^{+} + H_2O \rightarrow Ag^{\circ} + {}^{\cdot}OH + H^{+} \tag{6}$$

In Eq. (7), silver atoms formed by the irradiation from the relatively stabilised Ag clusters.

$$nAg^{\circ} \rightarrow (Ag^{\circ})n \tag{7}$$

where $(Ag^{\circ})_n$ is the silver nanocluster containing $n$ silver atoms. After the ultrasonic irradiation of the aqueous suspension of $AgNO_3$/*K. alvarezii*, many aqueous electrons ($e^{-}_{aq}$) were produced, and the $Ag^{+}$ ions were reduced into Ag-NPs.

Equation (8) shows a higher possibility for the single Ag atoms to nucleate and grow into $(Ag)_n$ clusters.

$$(Ag^{\circ})n \rightarrow (Ag^{\circ})_{n-1} + Ag^{+} \tag{8}$$

From the theory, this reaction had no substantial decrease in the particle size and changes in size distribution should be observed [26]. The agglomeration of these materials could also occur due to the high concentration of Ag-NPs.

This phenomenon will be clarified in the TEM images, which show the distribution and size particles. Moreover, the schematic illustration of the mechanism of *K. alvarezii* with Ag-NPs is depicted in Fig. 2. From this schematic, electrons from oxygen (seaweed *K. alvarezii*) have made a bonding under van der

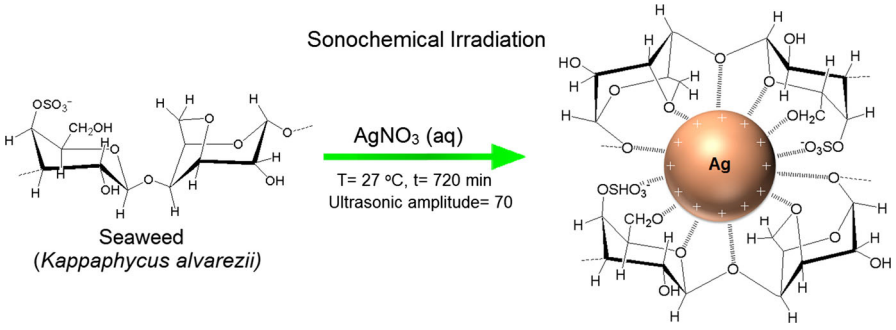


**Fig. 2** Schematic of synthesised Ag-NPs interactions with activated functional groups of seaweed *K. alvarezii*

Walls forces that stabilised in the capping of Ag-NPs. The FT-IR study will confirm the organic component responsible for the Ag-NP stabilisation.

The pH reaction was measured before and after ultrasound irradiation to study the effect of pH. A decrease in pH occurred from 6.15 before irradiation to 4.84 and 4.35 for 480 and 720 min of ultrasound irradiation, respectively. This pH could indicate the generation of $H^+$ ions during irradiation [27]. The condition of pH was in agreement with Eqs. 4, 5, and 6, in that $H^+$ ions were produced in the synthesis of Ag-NPs.

## UV–visible analysis

UV–visible spectroscopy data is a valuable tool to establish the formation of Ag-NPs because nanoparticle solution shows an absorption band in UV–vis range. UV–vis spectroscopy exhibits the SPR of the Ag electron and provides information on the size and shape of the nanoparticles [28]. As shown in Fig. 1, increasing irradiation time changed the colour of the solution from colourless to a dark brown and it effected the intensity of SPR from UV–vis spectra.

The UV–vis spectra was recorded until 720 min ultrasound irradiation in the synthesis of Ag-NPs, as displayed in Fig. 3. Before irradiation, no peak was observed between 300 and 800 nm. However, the peak appeared after 120 min irradiation due to SPR oscillation of Ag-NPs at 384 nm. The intensity increased with increasing time radiation, with significant change in its position.

As shown in Fig. 3a, when the irradiation time increases, the intensity of the SPR peaks also increases. These SPR bands arise due to the combined oscillations of the electrons of nanoparticles with visible light, and are influenced by the size and morphology of the nanoparticles [29].

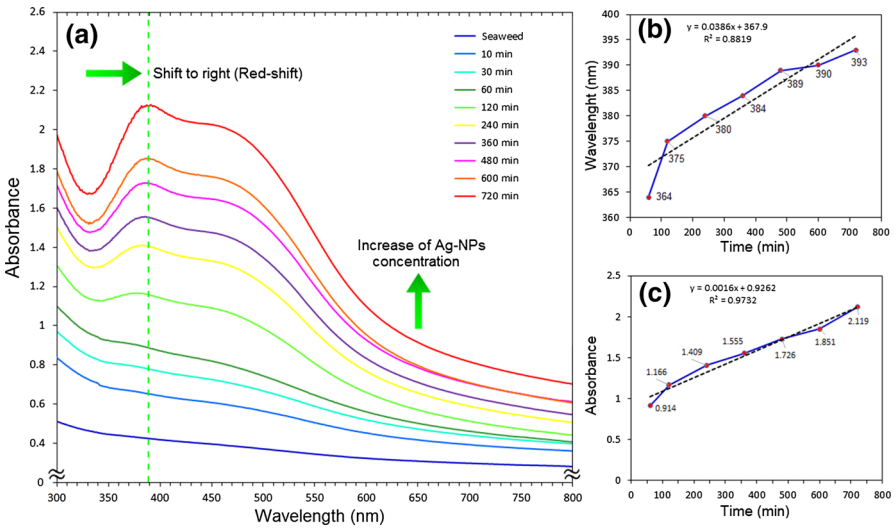


**Fig. 3** Time evolution of UV–vis absorption spectra for *K. alvarezii* and *K. alvarezii*/Ag-NPs, wavelength and absorbance (**b**, **c**), respectively

Figure 3b shows that with increasing time irradiation, absorbance also increases and shifts to a higher wavelength at 393 nm, to red-shift, which refers to an increase in the particle size [30]. This condition is suitable with Mei's theory that nanoparticles with different sizes should exhibit different optical properties due to the difference in SPR bands [31].

Figure 3c shoes that the sample with 720 min of irradiation time has a larger absorbance compared to the other samples. The increase of this absorbance indicates that the concentration of Ag-NPs has increased, and a higher concentration of metal nanoparticles may also lead to the red-shift of the SPR band [26, 32].

## X-ray diffraction pattern

This study gathers information about the crystalline nature of the synthesised nanoparticles. The XRD spectrum of *K. alvarezii* shown in Fig. 4a does not reveal any peaks, except at 21.51° due to the absence of silver. However, after irradiation until 720 min, Fig. 4b shows five diffraction peaks at 2θ values of 38.24°, 44.34°, 64.41°, 77.57°, and 81.87°.

The five diffraction peaks in this XRD pattern can be indexed by the face centre cubic (fcc). The structure of the silver was, respectively, to (111), (200), (220), (311), and (222) crystallographic planes ICDD/ICSD X'Pert High Score Plus (Ref. No. 01-087-0719). The XRD facets suggest that *K. alvarezii*/Ag-NPs is crystalline without apparent impurities [33, 34]. In addition, after calculating using the Debye–Scherrer (D) equation, the average *K. alvarezii*/Ag-NPs was estimated to be 13.14 nm, which was almost the same under TEM observation.

## Transmission electron microscopy study

The TEM image offers valuable information about the size and shape of the nanoparticles. The representative TEM images of Ag-NPs at different times are presented in Fig. 5a–c. The images suggest that the nanoparticles are almost

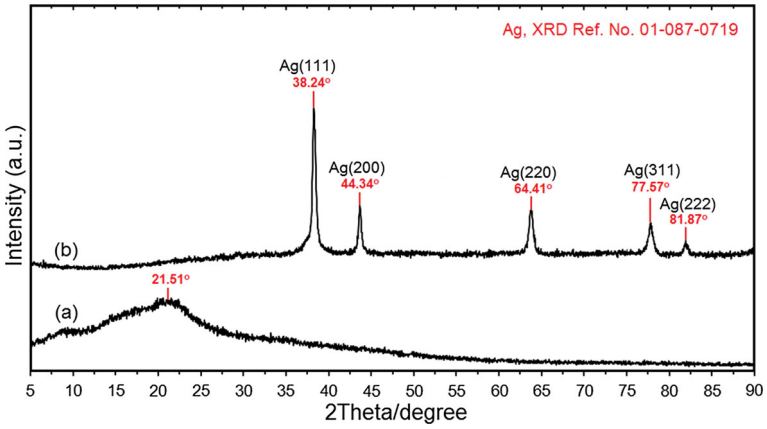


**Fig. 4** XRD Pattern of *K. alvarezii* (**a**) and *K. alvarezii*/Ag-NPs after 720 min (**b**) ultrasound irradiation

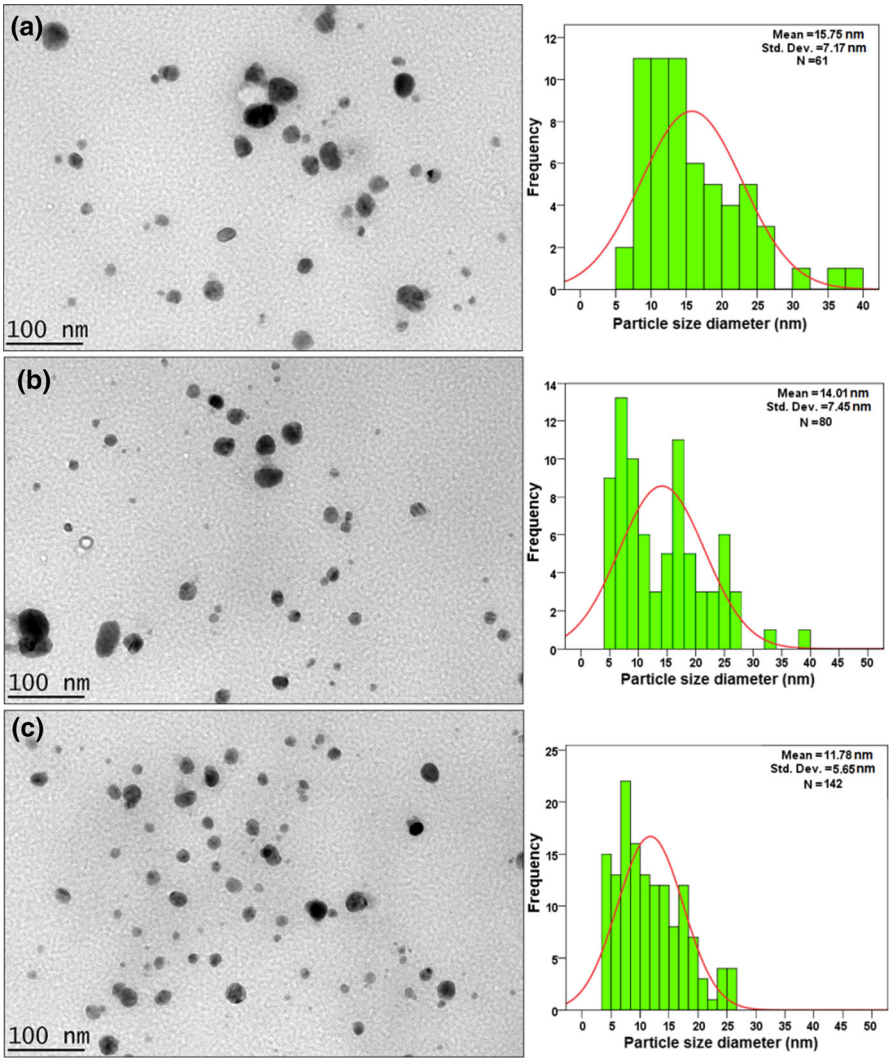


**Fig. 5** TEM images and particle size distribution of *K. alvarezii*/Ag-NPs at different ultrasound irradiation times [120, 480 and 720 min (**a**–**c**)]

spherical in shape. The histograms represent the size distribution of the particles, which have an average size of the particles of 15.75 ± 7.17, 14.01 ± 7.45, and 11.78 ± 5.65 nm after 120, 480 and 720 min of ultrasonic irradiation, respectively.

The number of Ag-NPs counts was around 61, 80, and 142 for 120, 480, and 720 min irradiation, respectively. These TEM results agree with the UV–vis spectral results, because of the similar effect of radiation time on the increasing distribution of nanoparticles. This growing distribution or concentration was related to the red-shift of the SPR. However, size decreased by irradiation time. Our data

indicated that when the ultrasound irradiation time was increased to 720 min, the concentration increased; however, the size reduced to 11.78 nm.

The size of nanoparticles in Fig. 5b after 480 min irradiation is 14.01 ± 7.45 nm. However, the size decreased to 11.78 ± 5.65 nm after 720 min in Fig. 5c. This unique phenomenon is related to the higher agglomeration of Ag-NPs after 720 min of irradiation. This condition increased the number or concentration of Ag-NPs and decreased their size. Disaggregation of Ag-NPs can be another reason for the decreased size of the nanoparticles [26].

## Field emission scanning electron microscopy with energy dispersive X-ray analysis

FESEM with EDX spectroscopy was used to determine the silver concentration of the nanoparticles. FESEM images of *K. alvarezii*/Ag-NPs are presented in Fig. 6a–c. Figure 6a represents *K. alvarezii* as the stabiliser before ultrasound irradiation.

Figure 6b and c show *K. alvarezii*/Ag-NPs after 480 and 720 min ultrasonic irradiation, respectively. Based on these images, the distributions of Ag-NPs were uniform and the shapes of Ag-NPs were spherical. This caused an increase in irradiation time to 480 min, and it improved to 720 min.

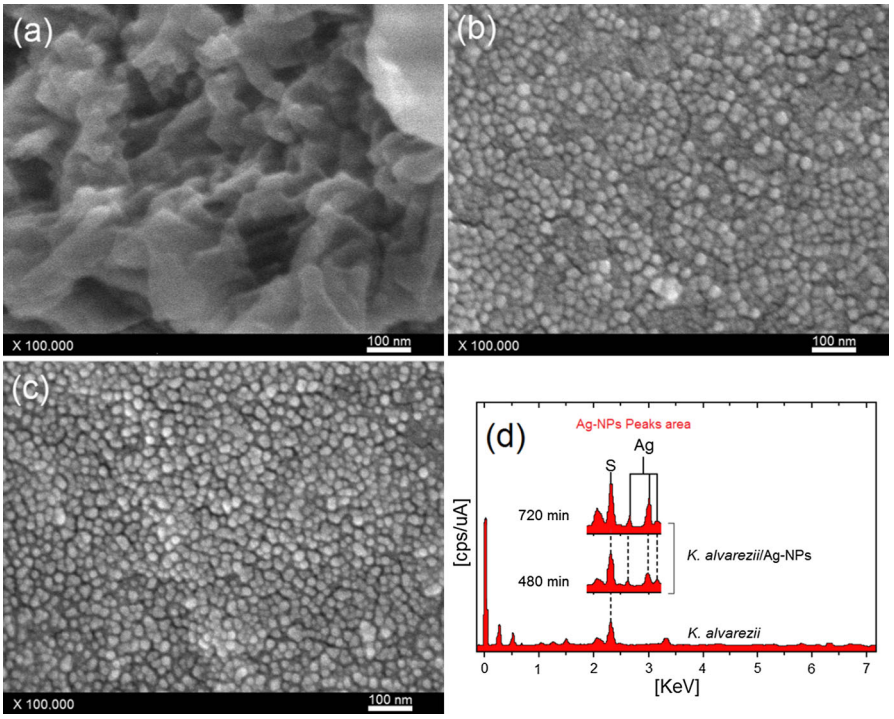


**Fig. 6** FESEM micrographs and EDX spectra for the *K. alvarezii* (**a**), and *K. alvarezii*/Ag-NPs after 480 min (**b**), 720 min (**c**) and EDX spectra (**d**)

The EDX spectra showed the characterised Ag-NPs in a particular absorption peak at approximately 3 keV. This absorption peak is due to the SPR phenomenon of the element Ag [35]. Figure 6d shows the EDX spectra for *K. alvarezii* and *K. alvarezii*/Ag-NPs after 480 and 720 min of ultrasonic irradiation. The peaks around 0.32, 0.51, 1.11, 1.25, 1.52, 2.28, 2.44, and 3.46 keV are related to the binding energies of seaweed *K. alvarezii*; and 2.68, 3.16, and 3.24 keV are associated with silver elements in *K. alvarezii*/Ag-NPs [36]. The percentages of nano-silver were 45.30 and 47.38 % after ultrasound irradiation for 480 and 720 min, respectively.

## Zeta potential analysis

The zeta potential analysis was performed to obtain information about the surface properties of the nanoparticles. This equipment can indicate the long-term stability of particulate systems. For a physically stable suspension stabilised by electrostatic repulsion, a zeta value of approximately ±30 mV is required. Moreover, in a combined electrostatic and steric stabilisation, ±20 mV is sufficient [37].

Zeta potential results have a negative value for *K. alvarezii* and *K. alvarezii*/Ag-NPs prepared after 480 and 720 min of ultrasonic irradiation (Fig. 7a–c). The zeta potential of *K. alvarezii* has a −42.39 mV value, whereas the *K. alvarezii*/Ag-NPs values after 480 and 720 min changed to −31.83 and −35.86 mV, as in Fig. 7a–c. Based on the required value for stability of solution (±30 mV), the *K. alvarezii*/Ag-NPs showed acceptable stability. The *K. alvarezii*/Ag-NPs after 480 and 720 min are gradually reduced then increased, however, not less than the required amount for stable expression, thereby producing stable *K. alvarezii*/Ag-NPs nanoparticles.

## Fourier transform infrared study

An FTIR measurement was performed to identify the possible biomolecules responsible for the stabilisation of the newly synthesised Ag-NPs. The FTIR spectrum for *K. alvarezii* and *K. alvarezii*/Ag-NPs after 480 and 760 min of ultrasound irradiation is presented in Fig. 8a–c. In *K. alvarezii*, the absorption peak at 3366 and 2919 $cm^{-1}$ could be assigned to the stretching vibrations of –OH and C–H groups [38].

The absorption band at 1638 $cm^{-1}$ could be attributed to the polymer-bond of water because water is the solvent, and the peak at 1410 $cm^{-1}$ was assigned to the sulphate stretching from the seaweed because *K. alvarezii* has many sulphate atoms in its chemical structure. The band at 1361 $cm^{-1}$ may be due to the methylene group bending from the seaweed. Thus, the intense band at 1213 $cm^{-1}$ could be assigned to O=S=O asymmetric stretching in *K. alvarezii*.

The two characteristic peaks at 1146 and 1122 $cm^{-1}$ were noticed to be S=O and C–O–C asymmetric stretching, respectively. The distinct peak at 1020 $cm^{-1}$ represented glycosidic linkage. The C–O–C stretching vibration of 3, 6-anhydro bridges could be associated with the peak at 917 $cm^{-1}$. In addition, the peak at 837 $cm^{-1}$ may be due to $C_4$–O–S stretching in B–D–galactose. Another band observed at 692, 565, and 380 $cm^{-1}$ was assigned to the stretching of S=O=S bending [39]. These peaks related to the chemical components from *K. alvarezii*.

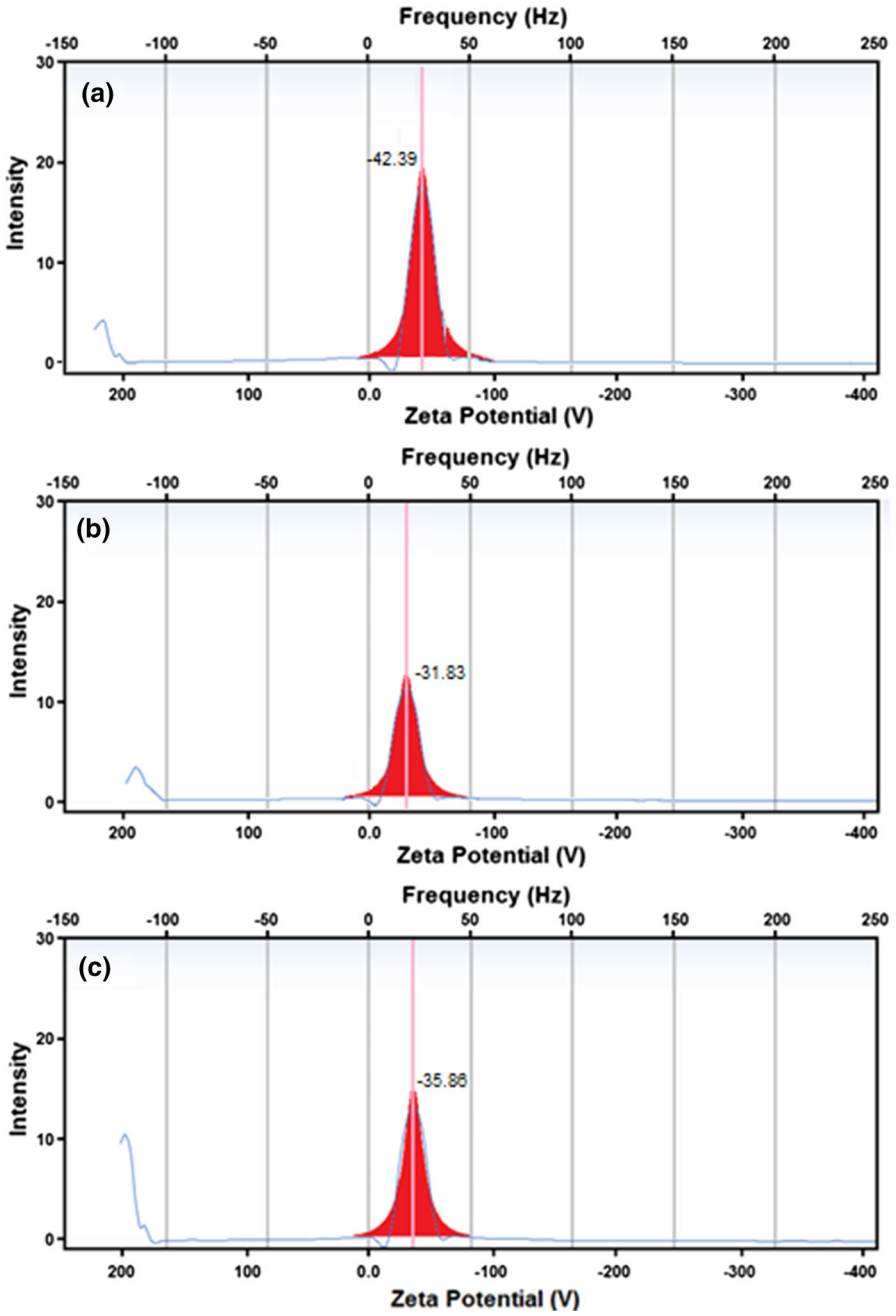


**Fig. 7** Zeta potential results for *K. alvarezii* (**a**), and *K. alvarezii*/Ag-NPs at different ultrasonic irradiation times: **b** 480 and **c** 720 min

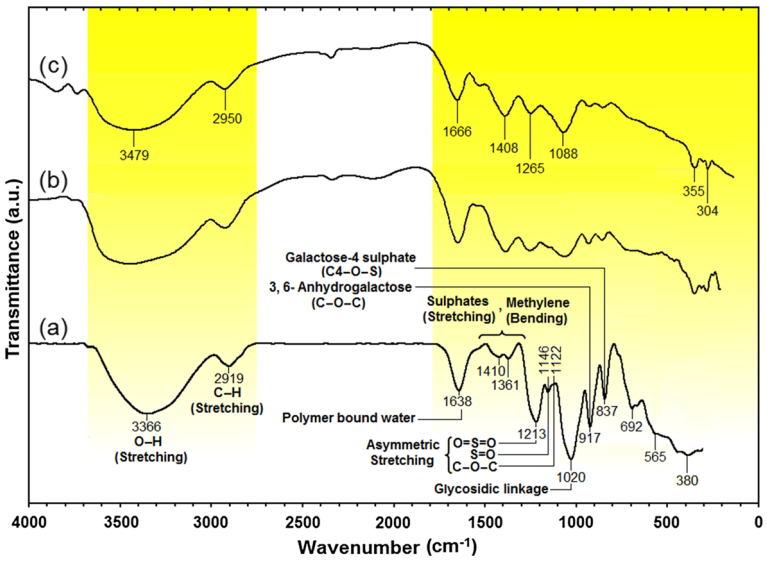


**Fig. 8** FTIR spectra for *K. alvarezii* (**a**), and *K. alvarezii*/Ag-NPs at different ultrasonic irradiation times: **b** 480 and **c** 720 min

The FTIR of *K. alvarezii*/Ag-NPs under 480 and 720 min shown in Fig. 8b–c had little that was different. The peak at 3479 and 2950 $cm^{-1}$ represents the stretching vibration of –OH and C–H groups, with more shifting due to the effect of irradiation [40]. Thus, the peak at 1638 $cm^{-1}$ shifted to 1666 $cm^{-1}$ represents the decreasing concentration of the polymer-bond of water, due to the low intensity of this peak.

The peak at 1410 $cm^{-1}$ did not record much shifting to 1408 $cm^{-1}$, due to insufficient interaction of sulphate stretching with the Ag-NPs. The peak at 1361 $cm^{-1}$ disappeared with increasing time until 720 min of irradiation. The peak at 1146 and 1122 $cm^{-1}$ also disappeared due to the intense irradiation from ultrasound, which broke the chemical structure of *K. alvarezii* as the bio-media.

The intensity of 1213 $cm^{-1}$ decreased and shifted to 1265 $cm^{-1}$ due to the decreasing concentration of O=S=O asymmetric stretching and the chemical bonding with the Ag-NPs, as shown in the schematic illustration in Fig. 2. The peak at 1020 $cm^{-1}$ of *K. alvarezii* shifted to 1088 $cm^{-1}$, and had low intensity due to glycosidic linkage decreasing from the seaweed.

Another peak with irradiation time at 355 and 304 $cm^{-1}$ indicated the stretching of S=O=S bending, and these peaks could be related to the production of Ag-NPs. The intensity and wavelength of peaks at different irradiations time both for 480 and 720 min followed an overall decrease. However, another new peak appeared at around 350 $cm^{-1}$, which indicates the presence of Ag-NPs.

The FTIR results confirmed that the *K. alvarezii* surface was capped by internal lone-pair oxygen atoms and sulphate groups from *K. alvarezii* as the bio-media. Indeed, TEM images from 480 and 720 min of irradiation also confirmed the presence of these nanoparticles. Stretching commonly occurs in polysaccharides

from natural stabiliser as the bio-media for Ag-NPs. These sulphate stretching vibrations are usable in the production of nanoparticles for stabilisation [23, 41].

This study is in agreement with Venkatpurwar et al. [19], who reported that sulphated polysaccharides isolated from the marine alga *Porphyra vietnamensis* had a substantial capacity to synthesise Ag-NPs. It is also consistent with the previous report from genus *Codium*, which is well known for containing polysaccharides.

## Conclusion

In this study, Ag-NPs were synthesised in an aqueous medium by using an ultrasound irradiation as reducing agent, using bio-media seaweed *K. alvarezii*. In the sonochemical route, colloidal Ag-NPs can be prepared by a green chemistry method using $AgNO_3$ as a silver precursor and *K. alvarezii* as a reducing and stabilising agent. Sonochemical reduction route demonstrates remarkable potential for fabricating the desired particle size and concentrations of colloidal Ag-NPs. Ultrasonic irradiation time, ultrasonic amplitude, and concentration of the metallic source and reducing agent are the main effective factors in size and yield of Ag-NPs. As ultrasonic irradiation time increases in high-intensity amplitude and cycle, Ag-NPs becomes smaller and their concentrations are enhanced.

**Acknowledgments** The authors would like to thank the Ministry of Education Malaysia for funding this research project through a Research University Grant of Universiti Teknologi Malaysia (UTM), with project title "Green sonochemical synthesis of silver nanoparticles using natural polymer media" and reference number PY/2015/04574 under PAS grant. We also thank the Research Management Centre (RMC) of UTM for providing an excellent research environment in which to complete this work.

## References

1. J.L. Gardea-Torresdey, E. Gomez, J.R. Peralta-Videa, J.G. Parsons, H. Troiani, M. Jose-Yacaman, Langmuir **19**(4), 1357 (2003)
2. C.K. Simi, T. Emilia Abraham, Bioprocess Biosyst. Eng. **30**(3), 173 (2007)
3. A. Safavi, G. Absalan, F. Bamdad, Anal. Chim. Acta **610**(2), 243 (2008)
4. A. Sugunan, C. Thanachayanont, J. Dutta, J.G. Hilborn, Sci. Technol. Adv. Mater. **6**(3–4), 335 (2005)
5. M. Rai, A. Yadav, A. Gade, Biotechnol. Adv. **27**(1), 76 (2009)
6. J.L. Elechiguerra, J.L. Burt, J.R. Morones, A. Camacho-, X. Gao, H.H. Lara, M.J. Yacaman, A. Camacho-Bragado, X. Gao, H.H. Lara, M.J. Yacaman, A. Camacho-, X. Gao, H.H. Lara, M.J. Yacaman, J. Nanobiotechnology **3**, 6 (2005)
7. J.S. Kim, E. Kuk, K.N. Yu, J.-H. Kim, S.J. Park, H.J. Lee, S.H. Kim, Y.K. Park, Y.H. Park, C.-Y. Hwang, Y.-K. Kim, Y.-S. Lee, D.H. Jeong, M.-H. Cho, Nanomed. Nanotechnol. Biol. Med. **3**(1), 95 (2007)
8. E. Hao, G.C. Schatz, J. Chem. Phys. **120**(1), 357 (2004)
9. A.D. McFarland, R.P. Van Duyne, Nano Lett. **3**(8), 1057 (2003)
10. D. Radziuk, D. Shchukin, H. Mohwald, J. Phys. Chem. C **112**, 2462 (2008)
11. K. Shameli, M. Bin Ahmad, W.M.Z.W. Yunus, N.A. Ibrahim, Y. Gharayebi, S. Sedaghat, Int. J. Nanomed. **5**(1), 1067 (2010)
12. K. Shameli, M. Bin Ahmad, W.M.Z.W. Yunus, A. Rustaiyan, N.A. Ibrahim, M. Zargar, Y. Abdollahi, Int. J. Nanomed. **5**(1), 875 (2010)
13. S. Joseph, B. Mathew, J. Mol. Liq. **204**, 184 (2015)
14. R.F. Elsupikhe, K. Shameli, M.B. Ahmad, Res. Chem. Intermed. **41**(11), 8829 (2015)

15. S. Patra, S. Mukherjee, A.K. Barui, A. Ganguly, B. Sreedhar, C.R. Patra, Mater. Sci. Eng., C **53**, 298 (2015)
16. Y. Nagata, Y. Watananabe, S. Fujita, T. Dohmaru, S. Taniguchi, J. Chem. Soc., Chem. Commun. **21**, 1620 (1992)
17. K. S. Suslick, G. J. Price, Applications of Ultrasound To Materials Chemistry. p. 295 (1999)
18. S. Li, Y. Shen, A. Xie, X. Yu, L. Qiu, L. Zhang, Q. Zhang, Green Chem. **9**(8), 852 (2007)
19. V. Venkatpurwar, V. Pokharkar, Mater. Lett. **65**(6), 999 (2011)
20. A.M. Salgueiro, A.L. Daniel-da-Silva, A.V. Girão, P.C. Pinheiro, T. Trindade, Chem. Eng. J. **229**, 276 (2013)
21. K.S. Kumar, K. Ganesan, P.V.S. Rao, Food Chem. **107**(1), 289 (2008)
22. A.L. Daniel-Da-Silva, J. Moreira, R. Neto, A.C. Estrada, A.M. Gil, T. Trindade, Carbohydr. Polym. **87**(1), 328 (2012)
23. M. Faried, K. Shameli, M. Miyake, H. Hara, N.B.A. Khairudin, Dig. J. Nanomater. Biostructures **10**(4), 1419 (2015)
24. V. Ganesan, A.D.J.A. Astalakshmi, P. Nima, A. Thangaraja. Int. J. Eng. Adv. Technol. **2**(5), 559 (2013)
25. C. He, L. Liu, Z. Fang, J. Li, J. Guo, J. Wei, Ultrason. Sonochem. **21**(2), 542 (2014)
26. M. Darroudi, M. Bin Ahmad, K. Shameli, A.H. Abdullah, N.A. Ibrahim, Solid State Sci. **11**(9), 1621 (2009)
27. R.A. Salkar, P. Jeevanandam, S.T. Aruna, Y. Koltypin, A. Gedanken, J. Mater. Chem. **9**, 1333 (1999)
28. M.A. Noginov, G. Zhu, M. Bahoura, J. Adegoke, C.E. Small, B.A. Ritzo, V.P. Drachev, V.M. Shalaev, Opt. Lett. **31**(20), 3022 (2006)
29. S. Link, M.A. El-Sayed, Annu. Rev. Phys. Chem. **54**(1), 331 (2003)
30. K. Shameli, M. Bin Ahmad, P. Shabanzadeh, E. A. J. Al-Mulla, A. Zamanian, Y. Abdollahi, S. D. Jazayeri, M. Eili, F. A. Jalilian, R. Z. Haroun, Res. Chem. Intermed., **40**(3), 1313 (2014)
31. J.R. Heath, Phys. Rev. B **40**(14), 9982 (1989)
32. M. Zargar, K. Shameli, G.R. Najafi, F. Farahani, J. Ind. Eng. Chem. **20**(6), 4169 (2014)
33. K. Shameli, M. Bin Ahmad, S. D. Jazayeri, P. Shabanzadeh, P. Sangpour, H. Jahangirian, Y. Gharayebi, Chem. Cent. J. **6**(1), 73 (2012)
34. J. Krstić, J. Spasojević, A. Radosavljević, M. Šiljegovć, Z. Kačarević-Popović, Radiat. Phys. Chem. **96**, 158 (2014)
35. T.N.V.K.V. Prasad, V.S.R. Kambala, R. Naidu, J. Appl. Phycol. **25**(1), 177 (2013)
36. C. Jacobs, R.H. Müller, Pharm. Res. **19**(2), 189 (2002)
37. M. Sen, E.N. Erboz, Food Res. Int. **43**(5), 1361 (2010)
38. H. Khanehzaei, M.B. Ahmad, K. Shameli, Z. Ajdari, M.A. Ghani, K. Kalantari, Res. Chem. Intermed. **41**(10), 7363 (2014)
39. M. Prodana, D. Ionita, C. Ungureanu, D. Bojin, I. Demetrescu, Dig. J. Nanomater. Biostructures **6**(2), 549 (2011)
40. R.R.R. Kannan, W.A. Stirk, J. Van Staden, S. Afr. J. Bot. **86**, 1 (2013)
41. K. Matsubara, M. Mori, H. Matsumoto, K. Hori, K. Miyazawa, J. Appl. Phycol. **15**(1), 87 (2001)